crystals

MDPI

Article

Structure of *Mycobacterium tuberculosis* 1-Deoxy-D-Xylulose 5-Phosphate Synthase in Complex with Butylacetylphosphonate

Victor Oliveira Gawriljuk [1], Rick Oerlemans [1], Robin M. Gierse [2,3], Riya Jotwani [1], Anna K. H. Hirsch [2,3] and Matthew R. Groves [1,*]

[1] Department of Drug Design, Groningen Research Institute of Pharmacy, University of Groningen, Antonius Deusinglaan 1, 9713 AV Groningen, The Netherlands; v.gawriljuk.ferraro.oliveira@rug.nl (V.O.G.); r.oerlemans@rug.nl (R.O.)
[2] Helmholtz Institute for Pharmaceutical Research Saarland (HIPS), Helmholtz Centre for Infection Research (HZI), Campus Building E8.1, 66123 Saarbrücken, Germany; robin.gierse@helmholtz-hips.de (R.M.G.); anna.hirsch@helmholtz-hips.de (A.K.H.H.)
[3] Department of Pharmacy, Saarland University, Campus Building E8.1, 66123 Saarbrücken, Germany
* Correspondence: m.r.groves@rug.nl

Abstract: Stagnation in the development of new antibiotics emphasizes the need for the discovery of drugs with novel modes of action that can tackle antibiotic resistance. Contrary to humans, most bacteria use the methylerythritol phosphate (MEP) pathway to synthesize crucial isoprenoid precursors. 1-deoxy-D-xylulose 5-phosphate synthase (DXPS) catalyzes the first and rate-limiting step of the pathway, making it an attractive target. Alkylacetylphosphonates (alkylAPs) are a class of pyruvate mimicking DXPS inhibitors that react with thiamin diphosphate (ThDP) to form a stable phosphonolactyl (PLThDP) adduct. Here, we present the first *M. tuberculosis* DXPS crystal structure in complex with an inhibitor (butylacetylphosphonate (BAP)) using a construct with improved crystallization properties. The 1.6 Å structure shows that the BAP adduct interacts with catalytically important His40 and several other conserved residues of the active site. In addition, a glycerol molecule, present in the D-glyceraldehyde 3-phosphate (D-GAP) binding site and within 4 Å of the BAP adduct, indicates that there is space to extend and develop more potent alkylAPs. The structure reveals the BAP binding mode and provides insights for enhancing the activity of alkylAPs against *M. tuberculosis*, aiding in the development of novel antibiotics.

Keywords: 1-deoxy-D-xylulose 5-phosphate synthase; MEP pathway; butylacetylphosphonate; antibiotics; *Mycobacterium tuberculosis*; DXPS; protein crystallography

check for updates

Citation: Gawriljuk, V.O.; Oerlemans, R.; Gierse, R.M.; Jotwani, R.; Hirsch, A.K.H.; Groves, M.R. Structure of *Mycobacterium tuberculosis* 1-Deoxy-D-Xylulose 5-Phosphate Synthase in Complex with Butylacetylphosphonate. *Crystals* **2023**, *13*, 737. https://doi.org/10.3390/cryst13050737

Academic Editor: Abel Moreno

Received: 30 March 2023
Revised: 20 April 2023
Accepted: 25 April 2023
Published: 27 April 2023

Copyright: © 2023 by the authors. Licensee MDPI, Basel, Switzerland. This article is an open access article distributed under the terms and conditions of the Creative Commons Attribution (CC BY) license (https://creativecommons.org/licenses/by/4.0/).

1. Introduction

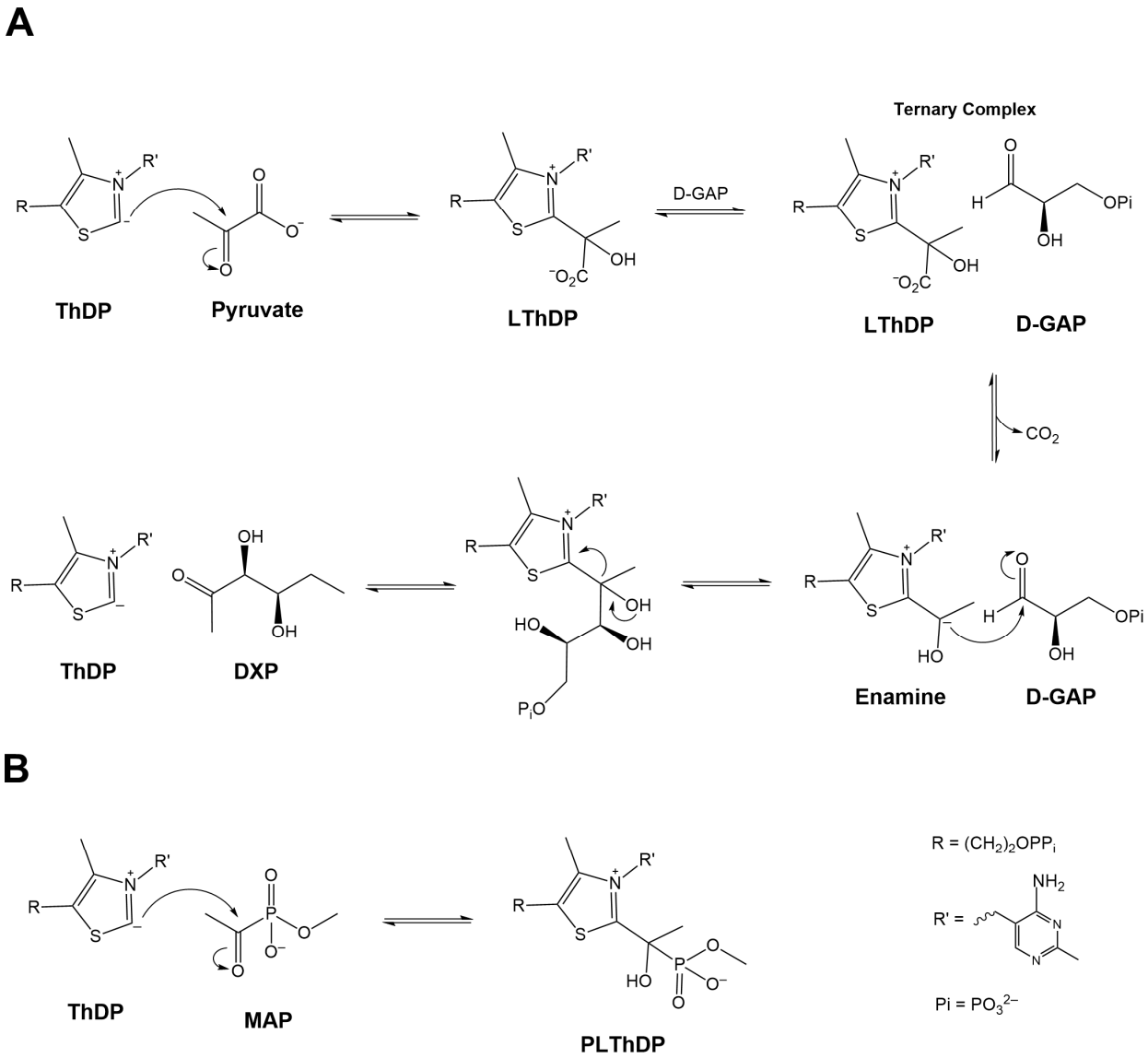
Antimicrobial resistance is a long and enduring problem in healthcare, with a global burden of 1.27 million deaths in 2019 [1]. Historically, resistance encouraged the development of new classes of antibiotics. However, nowadays, the problem persists but with reduced interest due to the low return on investment for the pharmaceutical industry [2–4]. The development of new antibiotics warrants not only the improvement of already known drugs, but most importantly, calls for the discovery of new scaffolds and the evaluation of un(der)explored targets [5,6].

The discovery of the methylerythritol phosphate (MEP) pathway for the synthesis of the universal isoprenoid precursors in bacteria provided new targets for the development of antibiotics [7,8]. Unlike humans, which use the mevalonate pathway for the synthesis of isopentenyl diphosphate (IDP) and dimethylallyl diphosphate (DMADP), the MEP pathway enzymes are unique targets with no human counterparts [9]. The 1-deoxy-D-xylulose 5-phosphate synthase (DXPS) is the first enzyme catalyzing the rate-limiting step of the MEP pathway [10]. The enzyme catalyzes the conversion of D-glyceraldehyde 3-phosphate (D-GAP) and pyruvate to 1-deoxy-D-xylulose 5-phosphate (DXP), a product

that is also used for the biosynthesis of thiamin and vitamin B6 [11–13]. As a branch point between essential pathways, DXPS is therefore an attractive target for the discovery of new antibiotics.

DXPS is a dimeric protein dependent on thiamin diphosphate (ThDP) as a cofactor for the reaction. However, divergent from other ThDP-dependent enzymes, the active site is not in the interface between the two dimers [14]. Additionally, instead of the ping-pong mechanism found in most ThDP-dependent enzymes, DXPS uses a random sequential reaction mechanism [15]. In this mechanism, the decarboxylation of the ThDP intermediate is induced through the presence of the second substrate.

In summary, the mechanism starts with pyruvate reacting with the thiazolium ring of ThDP to form a C2α-lactyl-ThDP (LThDP) intermediate. Afterwards, LThDP undergoes a D-GAP-induced decarboxylation, resulting in the production of enamine [16]. Finally, DXP is produced through the carboligation of D-GAP with enamine, releasing ThDP for a new cycle of reaction (Scheme 1A). The need for a stable ternary complex between LThDP and D-GAP for rapid decarboxylation makes DXPS unique among other ThDP-dependent enzymes, thus opening up space for the discovery of inhibitors that are selective for DXPS [11,16].



Scheme 1. (**A**) Reaction mechanism of DXPS. (**B**) Reaction mechanism of methylacetylphosphonate (MAP) inhibition.

Since its discovery as a target, inhibitors of DXPS have been developed using various strategies, including ThDP and substrate mimetics and competitors [8,11,17–20]. However, these inhibitors have had limited success due to their inability to achieve high selectivity and affinity for DXPS. As a result, there is still significant interest in identifying new scaffolds and strategies to improve inhibitor development for this target [11].

One approach that has been explored in the past involves the use of small alkylacetylphosphonates (alkylAPs) as inhibitors. MAP is an example of an alkylAP that has been used as a mechanistic probe for ThDP-dependent decarboxylases for a long time [21]. They are efficient inhibitors that covalently trap ThDP in a stable C2α-phosphonolactyl-ThDP (PLThDP) adduct, which mimics the pre-decarboxylation intermediate of the reaction (Scheme 1B). However, small alkylAPs such as MAP have limited selectivity for DXPS, making them unsuitable as DXPS inhibitors [21]. The unique characteristics found in DXPS such as a larger active site, acceptor substrate promiscuity and its different reaction mechanism enable the use of larger alkylAPs bearing hydrocarbon moieties that mimic both the pyruvate and acceptor substrate simultaneously. The use of larger alkylAPs allows for the development of more selective compounds with increased affinity against DXPS [22,23].

For instance, butylacetylphosphonate (BAP) was the first alkylAP showing high selectivity and inhibition of several DXPS homologues (*Escherichia coli*, *Mycobacterium tuberculosis*, *Yersina pestis* and *Salmonella enterica*) [22,24]. Afterwards, the compound was improved by extending the number of interactions mimicking the ternary complex. This second generation of alkylAPs showed 15,000 times more selectivity compared to other ThDP-dependent enzymes and submicromolar K_i values, highlighting the benefit of this approach [23].

We recently published the structure of a truncated construct of *M. tuberculosis* DXPS (ΔMtDXPS) and showed different stabilization mechanisms that could be used for the development of new antibiotics [25]. With the lack of DXPS structures in complex with inhibitors, we sought to use our system with improved crystallization properties to crystallize ΔMtDXPS with inhibitors known in the literature. BAP was chosen as a starting point due to its ready availability and broad-spectrum activity reported in multiple homologues. In addition, its unelaborated nature makes it an exemplary molecule for further structure-based design optimization of alkylAPs.

Here, we show the first ΔMtDXPS structure in complex with BAP. To our knowledge, this is the first DXPS structure in complex with an inhibitor that displays antimicrobial activity through the inhibition of DXPS. The structure sheds light on the BAP binding mode and gives structural insights that can guide the optimization of alkylAPs with increased activity against *M. tuberculosis*, contributing to the development of antibiotics with new modes of action.

2. Materials and Methods

2.1. Cloning

The MtDXPS truncation construct and expression vector used in this work was previously described in Gierse et al. [25].

2.2. ΔMtDXPS Expression and Purification

BL21-star (DE3) cells transformed with the pETM11–ΔMtDXPS vector were grown in LB media at 37 °C and 180 RPM, and were induced with 0.1 mM IPTG after reaching an OD_{600} of 0.6. After induction, the cells were grown for 16 h at 18 °C, and then were collected by centrifugation. The cell pellet was resuspended in lysis buffer (50 mM Tris pH 8, 350 mM NaCl, 20 mM imidazole, 10% glycerol, 1 mM DTT, 1 mM $MgCl_2$, 50 µg/mL Lysozyme and 10 µg/mL DNaseI). The cells were lysed with sonication and centrifuged at 41,000 g for 1 h to obtain the lysate.

The lysate was loaded on a HisTrap High-Performance 5 mL column (Cytiva, sourced from Fischer Scientific, Landsmeer, The Netherlands) pre-equilibrated with buffer A (50 mM Tris pH 8, 350 mM NaCl, 10% Glycerol and 20 mM imidazole). The column was washed

with 10 CV of buffer A and the protein was eluted with a gradient of buffer B (buffer A supplemented with 500 mM of imidazole) with an elution peak at 70% of buffer B. Fractions containing protein were pooled and the His-tag cleaved with the addition of a TEV protease, which was followed by overnight dialysis at 4 °C in dialysis buffer (50 mM Tris pH 8, 350 mM NaCl, 2 mM MgCl2, 500 µM ThDP and 1 mM DTT). The untagged protein was isolated with reverse affinity chromatography using the HisTrap column and further purified with a size-exclusion Superdex 75 16/60 HiLoad column (GE Healthcare, Hoevelaken, The Netherlands) pre-equilibrated with 20 mM Hepes pH 7.5, 150 mM NaCl, 5% glycerol, 5 mM $MgCl_2$ and 2 mM DTT. Protein fractions were concentrated to 4 mg/mL, flash-frozen in liquid nitrogen and stored at −80 °C for further use. Sample purity was assessed by SDS-PAGE.

2.3. Crystallization and Soaking

Prior to crystallization, ΔMtDXPS at 4 mg/mL was incubated with 2 mM of ThDP for two hours. After incubation, the crystals were grown using the sitting drop method at a 1:1 ratio using 0.1 M MES-imidazole pH 6.3, 10% PEG 8000 and 20% ethylene-glycol as the precipitant solution; crystals appeared after 7–14 days.

BAP–ΔMtDXPS crystals were obtained by soaking in 2 µL drops of precipitant solution supplemented with 1 mM BAP and 1 mM ThDP for 16 h. After soaking, the crystals were harvested and flash-frozen in liquid nitrogen for data collection.

2.4. Data Collection, Analysis and Refinement

Crystals were collected at the P11 beamline at the DESY facility using the fine ϕ-slicing method [26]. Data frames were further processed with XDS [27] and scaled and merged with Aimless [28]. The structures were solved by molecular replacement with Phaser [29] using the PDB coordinates 7A9H as the template model and were further refined using COOT [30] and phenix.refine [31]. Ligand restraints were generated with ACEDrug [32], which was implemented within the CCP4i2 [33] program suite. Polder maps were generated with phenix.polder using the standard parameters [34].The final structure was deposited in the Protein Data Bank with the accession code 8OGH.

2.5. Docking

SeeSAR version 12.1.0 (BioSolveIT GmbH, Sankt Augustin, Germany, 2022, www.biosolveit.de/SeeSAR, accessed on 27 January 2023) was used for docking BAP analogs. The BAP–ΔMtDXPS structure was used as the receptor, with the binding site being defined considering butyl PLThDP as the ligand. Only water molecules interacting with butyl PLThDP were maintained. The template docking mode was used with butyl PLThDP as the template ligand, while the atoms from the butyl moiety were removed to decrease template docking bias.

3. Results

3.1. Crystal Structure of ΔMtDXPS in Complex with BAP

We previously published a MtDXPS construct with a loop truncation that showed improved crystallization properties and enzyme kinetics similar to that of the wild type [25]. In this work we used the same construct to solve the structure of MtDXPS in complex with BAP. The BAP–ΔMtDXPS structure was obtained with a final resolution of 1.60 Å; the dataset and refinement statistics are shown in Table S1.

The asymmetric unit contains a homodimer with each subunit consisting of three distinct domains. Domain I (res 1–312) and domain II (res 313–483) contribute to the active site where ThDP is bound, whereas domain III (res 484–638) makes contact at the dimer interface (Figure 1). The regions from residues 177–232 and 288–314 are not observable in the electron density map. The first corresponds to the truncated loop, which is also not present in other DXPS structures, while the second one corresponds to the spoon and fork motif, which is only observed in the closed state of the enzyme [14,35]. The overall

structure is highly similar to that of the holo-ΔMtDXPS (C_α RMSD: 0.226) with only a small helix–helix loop (res. 37–41) that adopts a different orientation, likely due to the loop flexibility seen by the higher B-factor values in this region for all DXPS structures in the PDB.

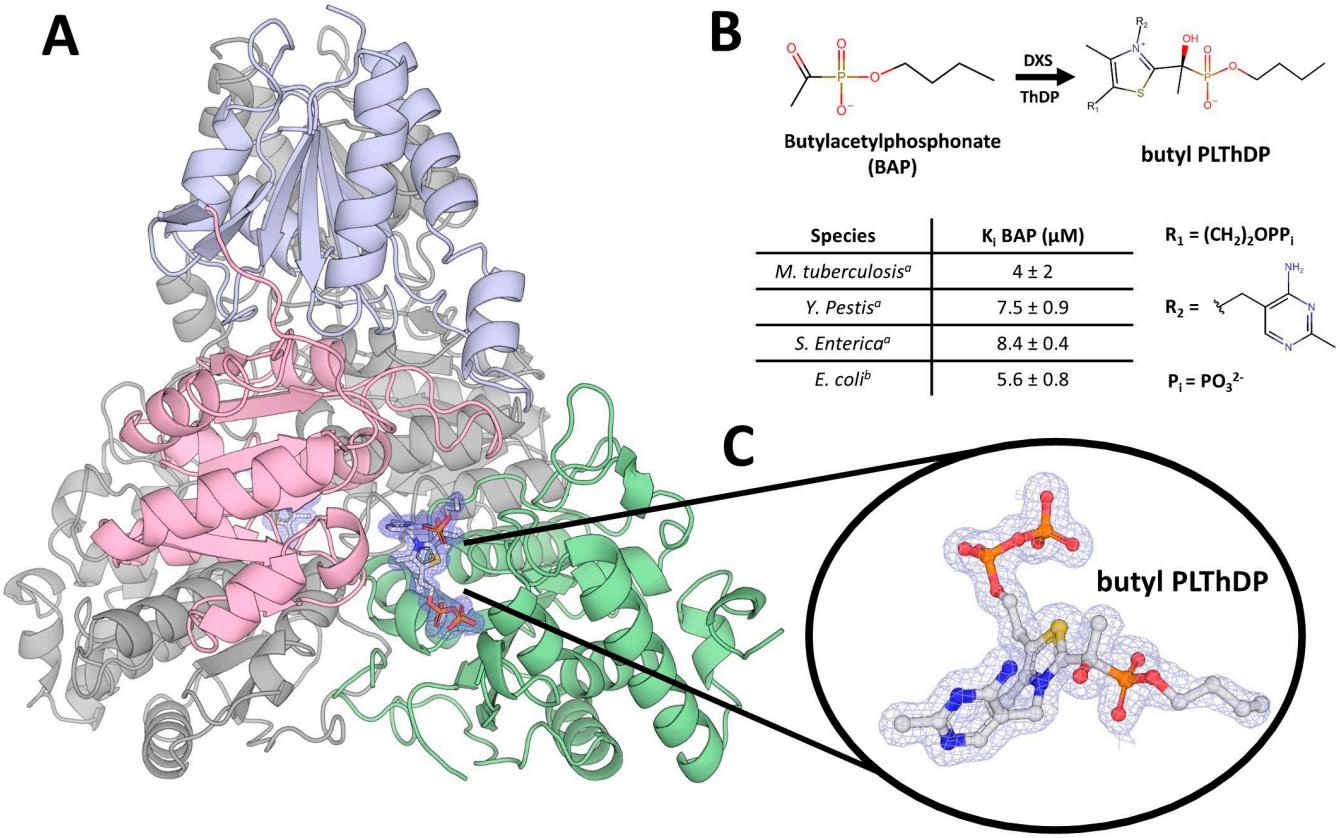


Figure 1. (**A**) Overview of the crystal structure of ΔMtDXPS in complex with BAP. Domain I (res 1–312), II (res 313–483) and III (res 483–638) are colored green, pink and blue, respectively. BAP reacts with ThDP to form a stable butyl PLThDP. (**B**) The table shows different K_i values described in the literature ([a]: values described in Smith et al. [24]; [b]: values described in Smith et al. [22]). (**C**) Stick representation of butyl PLThDP with 2Fo-Fc map density contoured at 1 σ in blue wire mesh.

3.2. Butyl Phosphonolactyl ThDP (Butyl PLThDP) Is Stabilized Similarly to PLThDP

Clear electron density for the butyl PLThDP can be seen in the active site of both chains confirming that, as expected, BAP reacts with ThDP to form a stable adduct (Figure 1B,C). The butyl PLThDP is stabilized similarly to the PLThDP in *Deinococcus radiodurans* DXPS (DrDXPS) [35]. The pyrimidine ring stacks with Phe390 to guarantee the correct orientation of the cofactor, allowing the N4′ amino group to interact with the main chain carbonyl of Ser112 and the C2α-hydroxyl group of the phosphonolactyl moiety. The phosphonates are further stabilized by a hydrogen bond with His40, which is known to be important for catalysis, [36] and a water-mediated hydrogen bond with His426 (Figure 2A,B). Finally, the butyl moiety adopts a linear structure with a less-defined electron density for the terminal carbons. The higher degree of freedom, together with the extended DXPS active site, can explain the flexibility and lack of clear density for those atoms.

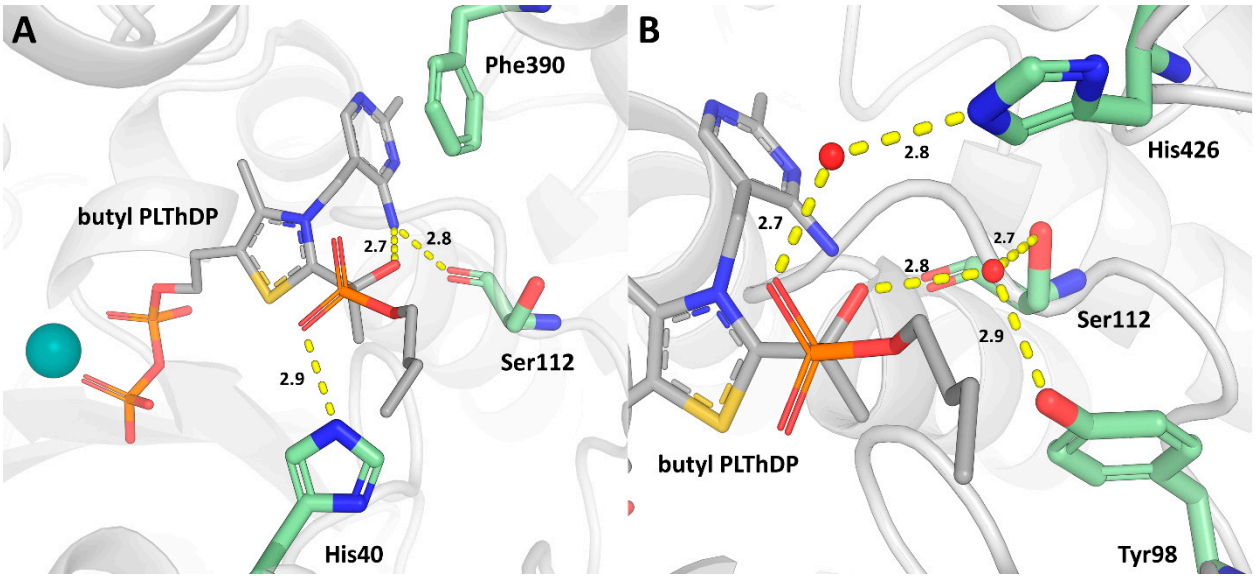


Figure 2. Active site of ΔMtDXPS with butyl PLThDP. (**A**) Pyrimidine ring and phosphonolactyl interactions with residues of the active site highlighted in green. (**B**) Hydrogen bond network of C2α-hydroxyl with residues highlighted in green and water molecules represented as red spheres. Hydrogen bonds are shown as dashed lines with distances in Angstroms.

3.3. ΔMtDXPS Uses a Water Molecule as a Replacement in the Interaction between His426 and the C2α-Hydroxyl

In addition to the hydrogen bonds with the N4′ amino group, the C2α-hydroxyl also interacts with one water molecule that makes a network of hydrogen bonds with Tyr98 and Ser112. In the enamine intermediate and PLThDP structures of DrDXPS, the C2α-hydroxyl is stabilized through His434 [35]. However, in MtDXPS the respective histidine (His426) is in a different conformation that does not allow for the same interaction due to the steric restriction imposed by Ser112.

We have previously shown that the same water molecule causes similar interactions with the C2α-hydroxyl of the ΔMtDXPS enamine intermediate [25]. This suggests that the water molecule might play a role in replacing His426 to stabilize the post-decarboxylation steps of the reaction, due to the different conformation of this residue in ΔMtDXPS. Interestingly, in the butyl PLThDP structure His426 does not take part in this hydrogen bond network due to interactions with another water molecules that stabilize the phosphonate (Figure 2B).

3.4. Glycerol Molecule in the Active Site Highlights the GAP Binding Site as a Target for alkylAP Optimization

Interestingly, a clear density for a glycerol molecule was found in Chain A close to the GAP binding site. Polder maps were calculated to confirm that the densities were not bulk solvent. The residues that are in proximity to the glycerol molecule are Arg415, His426, Lys473 and Tyr387. Lys473 is not found to interact with glycerol even though it is part of the GAP binding site. It is present in a different conformation, being orientated outside of the active site. The only residue that interacts with glycerol is Arg415 (Figure 3).

The presence of butyl PLThDP and additional molecules emphasizes that the large active site can be used to develop molecules that are more selective for DXPS simply by extending the alkylAPs to reach the GAP binding site. The distance between the butyl PLThDP and the glycerol molecule is 4 Å; therefore, linkers of 2–3 carbons might already be enough to link the two regions (Figure 3).

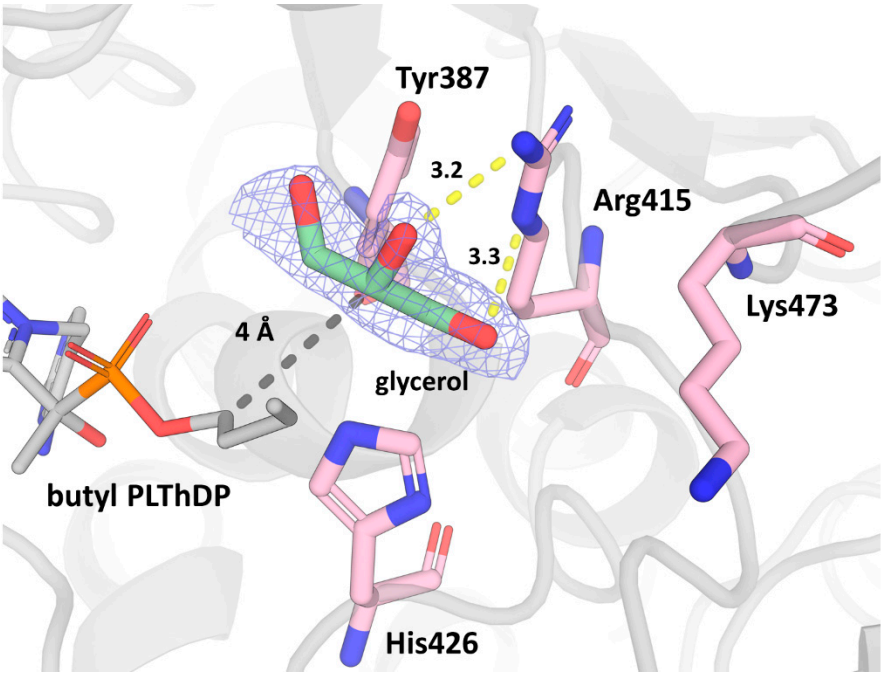


Figure 3. ΔMtDXPS GAP binding site with Polder map density contoured at 4 σ in blue wire mesh for the glycerol molecule. Residues of the GAP binding site are shown as stick representation and colored in pink. Hydrogen bonds are represented as yellow dashed lines, with distances represented in Angstroms.

3.5. Docking Second-Generation alkylAPs

One example of how this strategy can be successful is the second generation of alkylAPs, which was previously reported for *E. coli*. These compounds were optimized by extending BAP to reach the GAP binding side, thus mimicking the ternary complex of the enzyme [23]. While minor differences in the active sites of the DXPS homologs of *E. coli* and *M. tuberculosis* exist, the presented model of BAP in complex with MtDXPS allows us to assess whether similar improvements in affinity may also be achievable for inhibitors of the mycobacterial homolog. In order to potentially gain some insight into the binding mode of these compounds in *M. tuberculosis*, we docked D-PheTrAP, one of the more potent compounds from the second generation of alkylAPs, against EcDXPS (Figure 4). As a common mechanism of alkylAPs, D-PheTrAP reacts with ThDP to form a covalent adduct that inhibits the enzyme. Therefore, the predicted covalent adduct of D-PheTrAP with ThDP was used as a molecule for the docking studies.

Most docking poses were similar, with the carboxylic acid moiety interacting with the GAP binding site and only the phenyl ring adopting different conformations. The carboxylic acid group interacts with Arg415 similarly to glycerol, while the 1,2,3-triazole ring links the other groups to the GAP binding site (Figure 4). Lys473 was not shown to interact with the docked molecule, likely due to its orientation facing out of the active site in the BAP-bound structure. Flexible docking, by sampling the conformational space of Lys473, was performed using smina [37] to confirm that the residue can change its conformation to interact with the compound. Poses similar to the previous one were obtained via Lys473 interacting with the carboxylic moiety and Arg415 making close contact (Figure S1). In agreement with the observed improvement of affinity between BAP and D-PheTrap for *E. coli* DXPS, the predicted binding energies of BAP and D-PheTrap were −7.4 kcal/mol and −8.2 kcal/mol, respectively. However, calculated binding energies from docking approaches should be treated with caution as they can be unreliable due to the scoring functions implemented, making comparisons between different molecules based purely on energies somewhat unreliable.

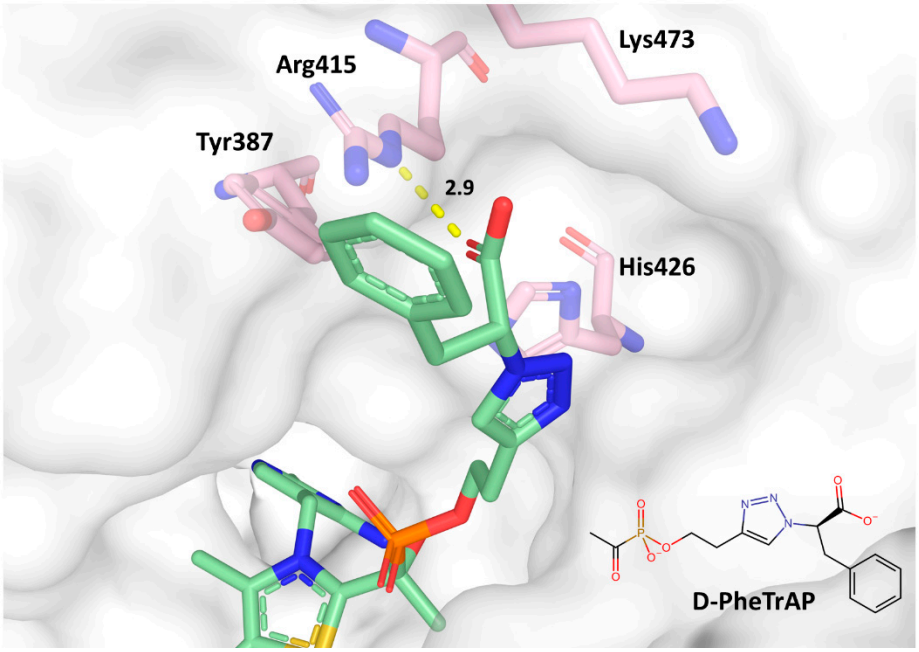


Figure 4. Docking of the covalent adduct of D-PheTrAP with ThDP to the active site of ΔMtDXPS structure. The pose with the highest affinity docking score is represented with green sticks, while residues of the GAP binding site are colored in pink. Hydrogen bonds are represented as yellow dashed lines, with distances indicated in Angstroms.

The flexibility of Lys473 is further supported by our previous structure with a bound phosphate where, in the presence of this negatively charged molecule, the residue adopts a different conformation that interacts with phosphate (Figure 5) [25]. Therefore, this indicates that the lysine residue can adopt multiple conformations, giving rise to the possibility that it can also contribute to the binding of potential inhibitors.

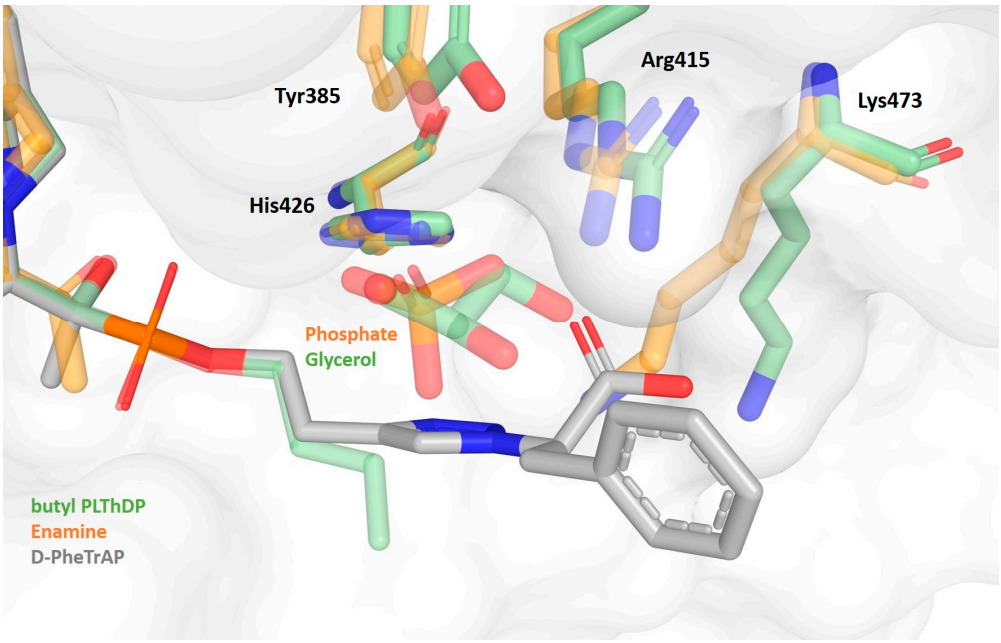


Figure 5. Superposition of docked molecule in the MtDXPS active site of the BAP- and enamine-bound structures (PDBID 7A9G). Residues of the BAP-bound structure are highlighted as opaque green sticks. Residues of the enamine-bound structure are highlighted as transparent orange sticks. The docked molecule is represented as gray sticks.

The superposed structures also show that glycerol and phosphate occupy similar positions in the GAP binding site, with Tyr 385 and Arg 415 in a comparable orientation. Despite the similarities in the position of the two molecules, in the presence of a more polar/negatively charged molecule, Lys473 seems to move and adopt a conformation closer to that of ThDP. In the docking poses obtained, the carboxylic acid group is not in a similar position to glycerol or phosphate, suggesting the linker between the phosphonolactyl moiety can be optimized to improve its position.

4. Discussion

DXPS catalyzes the first and rate-limiting step of the MEP pathway and is an important branch point for the synthesis of thiamin-related biomolecules such as vitamin B1 and B6, making this enzyme an attractive target for the development of new antibiotics [10,12,13]. Here, we present the structure of ΔMtDXPS in complex with BAP, allowing not only for the study of the binding mode of the ligand, but also providing new information for the future development of new alkylAP analogs. While expected based on sequence conservation, the experimentally confirmed similarity of the MtDXPS active site and mode of interaction with BAP with that seen in the DXPS of other organisms allows for the leveraging of a later generation of BAP-based compounds to be directly applied towards the development of antitubercular therapies.

BAP was the first alkylAP with selective inhibition towards DXPS, showing that the larger active site and substrate promiscuity could be used as an advantage to avoid targeting other ThDP-dependent enzymes [22]. The ΔMtDXPS structure in complex with BAP shows that the stabilization of the final adduct is similar to what was previously described for the PLThDP complex with DrDXPS [35]. Since PLThDP is a mimic of the pre-decarboxylation intermediate, the residues that interact with butyl PLThDP are conserved among DXPS enzymes' of different species. Therefore, BAP and alkylAPs, in general, are good candidates for the development of a universal DXPS inhibitor, which could be used not only to treat bacterial infections, but also other infective agents such as malaria caused by *Plasmodium falciparum*.

When compared with the structure of DrDXPS in complex with MAP, the addition of more carbons does not seem to impact the orientation or interactions with the C2α-phosphonolactyl [35]. Previous studies have shown that alkyl extensions in acetylphosphonates with aliphatic chains up to eight carbons long could still maintain similar potency in EcDXPS [38]. The space available in the active site and the similar stabilization of the C2α-phosphonolactyl seen in both structures could explain the conservation of potency even when larger alkyl substituents are used.

The ΔMtDXPS–BAP structure is in an open conformation, causing the active site to be completely exposed to the solvent. Hydrogen–deuterium exchange MS studies have shown that upon D-GAP binding a shift in the conformational equilibrium to the open state appears to occur, increasing the decarboxylation rate for the next step of the reaction [16,39]. Therefore, it is expected that the second generation of alkylAPs, which were designed to mimic the ternary complex, would target the open state of the enzyme.

As an example, the docking studies performed with one of the most potent compounds of the second generation previously reported to inhibit EcDXPS suggest that D-PheTrAP is also likely to inhibit MtDXPS. Even though Lys473 is pointing towards the outside of the active site in the structure herein obtained, flexible docking and previous structures indicate that the residue is flexible and can change its position to contribute to the interactions with the compound. This is further supported by the fact that mutational studies of Arg480, the analog of Lys473 in EcDXPS, showed that replacing it with alanine had a negative impact on both D-GAP Km and the inhibitory potency of D-PheTrAP in EcDXPS [23]. Since the D-GAP K_m is similar in both EcDXPS and MtDXPS, it is likely that Lys473 fulfils a similar role as Arg480 in EcDXPS [15,22].

The butyl PLThDP–MtDXPS structure can be leveraged to find the best options to extend the alkylAPs towards the GAP binding site. Glycerol and butyl PLThDP can be

used as anchor points to probe scaffolds that can interact with the GAP binding site, in addition to being used as linker options to connect the two regions. In order to achieve this, new strategies such as chemical space docking can be leveraged to guarantee the synthetic feasibility and optimal ADME properties of the predicted molecules [40].

For now, the use of a truncation strategy seems a necessary evil to obtain high-resolution, reproducible crystal structures of MtDXPS. The impact of the loop truncation on the obtained conformational state of the protein and the binding mode of butyl PLThDP is, as yet, unknown. However, due to the absence of a clearly interpretable density of this loop in other holo- or MAP-bound structures of homologues, it is unlikely that it would cause significant changes in the BAP binding mode [14,35,41]. The similarity in kinetics between the truncated enzyme and the WT provides additional evidence for this argument [25,42].

Due to the benefits of high-resolution data and reproducible crystallization, the truncation strategy opens up the possibility of using innovative methods for the development of new alkylAPs [25,42]. For example, X-ray-based fragment screening can be performed to probe fragments or scaffolds that are able to interact with the GAP binding site in the presence of ThDP or the butyl PLThDP intermediate [43,44]. Those fragments could later be linked in a similar way to that used in the design of the second generation of alkylAPs [23].

The increase in antibiotic resistance, together with its negative impacts on the healthcare system, necessitates the urgent development of antibiotics with new mechanisms of action. AlkylAPs are a promising strategy for the selective inhibition of DXPS, with peptidic pro-drug molecules already being developed to increase their uptake in bacterial cells [45]. We believe that the results obtained herein can contribute to the development of new analogs using structure-based strategies that were not previously available.

Supplementary Materials: The following supporting information can be downloaded at: https://www.mdpi.com/article/10.3390/cryst13050737/s1, Table S1: Summary of data collection and refinement statistics; Figure S1: Flexible docking pose of the covalent adduct of D-PheTrAP with ThDP. The docking pose is shown as green sticks. Residues of the MtDXPS structure with the new Lys473 orientation are coloured in pink, while the original Lys473 orientation is highlighted as white sticks. Hydrogen bonds are represented as yellow dashed lines, with distances indicated in Angstroms. Distances are represented as black dashed lines, with distances indicated in Angstroms.

Author Contributions: Conceptualization, M.R.G.; methodology, V.O.G., R.J., R.O. and R.M.G.; validation, V.O.G., R.O. and M.R.G.; formal analysis, V.O.G. and R.O.; investigation, V.O.G.; resources, M.R.G. and A.K.H.H.; data curation, V.O.G., R.O. and M.R.G.; writing—original draft preparation, V.O.G. and R.O.; writing—review and editing, all authors; visualization, V.O.G. and R.O.; supervision, M.R.G.; project administration, M.R.G. and A.K.H.H.; funding acquisition, A.K.H.H. and M.R.G. All authors have read and agreed to the published version of the manuscript.

Funding: This research was funded by the European Union's Horizon 2020 research and innovation programme under the Marie Sklodowska-Curie Grant Agreement No. 860816, as well as by The Netherlands Organisation for Scientific Research (NWO), LIFT Grant 731.015.414.

Data Availability Statement: The ΔMtDXPS–BAP structure and electron density maps were deposited in the Protein Data Bank under the accession code PDB: 8OGH.

Acknowledgments: We thank Caren Freel Meyers for kindly providing the butylacetylphosphonates for the experiments. We also would like to acknowledge DESY (Hamburg, Germany), a member of the Helmholtz Association HGF, for providing the experimental facilities. Parts of this research were carried out at PETRA III, and we would like to thank the P11 beamline staff for assistance in using their beamline. Beamtime was allocated for 20211417.

Conflicts of Interest: The authors declare no conflict of interest.

References

1. Murray, C.J.; Ikuta, K.S.; Sharara, F.; Swetschinski, L.; Robles Aguilar, G.; Gray, A.; Han, C.; Bisignano, C.; Rao, P.; Wool, E.; et al. Global Burden of Bacterial Antimicrobial Resistance in 2019: A Systematic Analysis. *Lancet* **2022**, *399*, 629–655. [CrossRef] [PubMed]
2. Plackett, B. No Money for New Drugs. *Nat. Outlook* **2020**, *586*, 50–52.

3. Ventola, C.L. The Antibiotic Resistance Crisis: Part 1: Causes and Threats. *Pharm. Ther.* **2015**, *40*, 277–283.
4. Theuretzbacher, U.; Baraldi, E.; Ciabuschi, F.; Callegari, S. Challenges and Shortcomings of Antibacterial Discovery Projects. *Clin. Microbiol. Infect. Off. Publ. Eur. Soc. Clin. Microbiol. Infect. Dis.* **2022**, *29*, 610–615. [CrossRef]
5. Miethke, M.; Pieroni, M.; Weber, T.; Brönstrup, M.; Hammann, P.; Halby, L.; Arimondo, P.B.; Glaser, P.; Aigle, B.; Bode, H.B.; et al. Towards the Sustainable Discovery and Development of New Antibiotics. *Nat. Rev. Chem.* **2021**, *5*, 726–749. [CrossRef]
6. Spellberg, B. The Future of Antibiotics. *Crit. Care* **2014**, *18*, 228. [CrossRef] [PubMed]
7. Rohmer, M. The Discovery of a Mevalonate-Independent Pathway for Isoprenoid Biosynthesis in Bacteria, Algae and Higher Plants. *Nat. Prod. Rep.* **1999**, *16*, 565–574. [CrossRef]
8. Masini, T.; Hirsch, A.K.H. Development of Inhibitors of the 2C-Methyl-D-Erythritol 4-Phosphate (MEP) Pathway Enzymes as Potential Anti-Infective Agents. *J. Med. Chem.* **2014**, *57*, 9740–9763. [CrossRef]
9. Lombard, J.; Moreira, D. Origins and Early Evolution of the Mevalonate Pathway of Isoprenoid Biosynthesis in the Three Domains of Life. *Mol. Biol. Evol.* **2010**, *28*, 87–99. [CrossRef]
10. Estévez, J.M.; Cantero, A.; Reindl, A.; Reichler, S.; León, P. 1-Deoxy-D-Xylulose-5-Phosphate Synthase, a Limiting Enzyme for Plastidic Isoprenoid Biosynthesis in Plants. *J. Biol. Chem.* **2001**, *276*, 22901–22909. [CrossRef]
11. Bartee, D.; Freel Meyers, C.L. Toward Understanding the Chemistry and Biology of 1-Deoxy-D-Xylulose 5-Phosphate (DXP) Synthase: A Unique Antimicrobial Target at the Heart of Bacterial Metabolism. *Acc. Chem. Res.* **2018**, *51*, 2546–2555. [CrossRef]
12. Du, Q.; Wang, H.; Xie, J. Thiamin (Vitamin B1) Biosynthesis and Regulation: A Rich Source of Antimicrobial Drug Targets? *Int. J. Biol. Sci.* **2011**, *7*, 41–52. [CrossRef] [PubMed]
13. Sprenger, G.A.; Schörken, U.; Wiegert, T.; Grolle, S.; de Graaf, A.A.; Taylor, S.V.; Begley, T.P.; Bringer-Meyer, S.; Sahm, H. Identification of a Thiamin-Dependent Synthase in *Escherichia Coli* Required for the Formation of the 1-Deoxy-D-Xylulose 5-Phosphate Precursor to Isoprenoids, Thiamin, and Pyridoxol. *Proc. Natl. Acad. Sci. USA* **1997**, *94*, 12857–12862. [CrossRef] [PubMed]
14. Xiang, S.; Usunow, G.; Lange, G.; Busch, M.; Tong, L. Crystal Structure of 1-Deoxy-D-Xylulose 5-Phosphate Synthase, a Crucial Enzyme for Isoprenoids Biosynthesis. *J. Biol. Chem.* **2007**, *282*, 2676–2682. [CrossRef]
15. Brammer, L.A.; Smith, J.M.; Wades, H.; Meyers, C.F. 1-Deoxy-D-Xylulose 5-Phosphate Synthase Catalyzes a Novel Random Sequential Mechanism. *J. Biol. Chem.* **2011**, *286*, 36522–36531. [CrossRef] [PubMed]
16. Patel, H.; Nemeria, N.S.; Brammer, L.A.; Freel Meyers, C.L.; Jordan, F. Observation of Thiamin-Bound Intermediates and Microscopic Rate Constants for Their Interconversion on 1-Deoxy-D-Xylulose 5-Phosphate Synthase: 600-Fold Rate Acceleration of Pyruvate Decarboxylation by D-Glyceraldehyde-3-Phosphate. *J. Am. Chem. Soc.* **2012**, *134*, 18374–18379. [CrossRef] [PubMed]
17. Zhu, D.; Johannsen, S.; Masini, T.; Simonin, C.; Haupenthal, J.; Illarionov, B.; Andreas, A.; Awale, M.; Gierse, R.M.; van der Laan, T.; et al. Discovery of Novel Drug-like Antitubercular Hits Targeting the MEP Pathway Enzyme DXPS by Strategic Application of Ligand-Based Virtual Screening. *Chem. Sci.* **2022**, *13*, 10686–10698. [CrossRef]
18. Johannsen, S.; Gierse, R.M.; Olshanova, A.; Smerznak, E.; Laggner, C.; Eschweiler, L.; Adeli, Z.; Hamid, R.; Alhayek, A.; Reiling, N.; et al. Not Every Hit-Identification Technique Works on 1-Deoxy-D-Xylulose 5-Phosphate Synthase (DXPS): Making the Most of a Virtual Screening Campaign. *ChemMedChem* **2023**, e202200590. [CrossRef]
19. Marcozzi, A.; Masini, T.; Zhu, D.; Pesce, D.; Illarionov, B.; Fischer, M.; Herrmann, A.; Hirsch, A.K.H. Phage Display on the Anti-Infective Target 1-Deoxy-D-Xylulose-5-Phosphate Synthase Leads to an Acceptor–Substrate Competitive Peptidic Inhibitor. *ChemBioChem* **2018**, *19*, 58–65. [CrossRef]
20. Jumde, R.P.; Guardigni, M.; Gierse, R.M.; Alhayek, A.; Zhu, D.; Hamid, Z.; Johannsen, S.; Elgaher, W.A.M.; Neusens, P.J.; Nehls, C.; et al. Hit-Optimization Using Target-Directed Dynamic Combinatorial Chemistry: Development of Inhibitors of the Anti-Infective Target 1-Deoxy-D-Xylulose-5-Phosphate Synthase. *Chem. Sci.* **2021**, *12*, 7775–7785. [CrossRef]
21. O'Brien, T.A.; Kluger, R.; Pike, D.C.; Gennis, R.B. Phosphonate Analogues of Pyruvate. Probes of Substrate Binding to Pyruvate Oxidase and Other Thiamin Pyrophosphate-Dependent Decarboxylases. *Biochim. Biophys. Acta* **1980**, *613*, 10–17. [CrossRef] [PubMed]
22. Smith, J.M.; Vierling, R.J.; Meyers, C.F. Selective Inhibition of *E. coli* 1-Deoxy-D-Xylulose-5-Phosphate Synthase by Acetylphosphonates. *Medchemcomm* **2012**, *3*, 65–67. [CrossRef] [PubMed]
23. Bartee, D.; Freel Meyers, C.L. Targeting the Unique Mechanism of Bacterial 1-Deoxy-D-Xylulose-5-Phosphate Synthase. *Biochemistry* **2018**, *57*, 4349–4356. [CrossRef]
24. Smith, J.M.; Warrington, N.V.; Vierling, R.J.; Kuhn, M.L.; Anderson, W.F.; Koppisch, A.T.; Freel Meyers, C.L. Targeting DXP Synthase in Human Pathogens: Enzyme Inhibition and Antimicrobial Activity of Butylacetylphosphonate. *J. Antibiot.* **2014**, *67*, 77–83. [CrossRef]
25. Gierse, R.M.; Oerlemans, R.; Reddem, E.R.; Gawriljuk, V.O.; Alhayek, A.; Baitinger, D.; Jakobi, H.; Laber, B.; Lange, G.; Hirsch, A.K.H.; et al. First Crystal Structures of 1-Deoxy-D-Xylulose 5-Phosphate Synthase (DXPS) from Mycobacterium Tuberculosis Indicate a Distinct Mechanism of Intermediate Stabilization. *Sci. Rep.* **2022**, *12*, 7221. [CrossRef]
26. Mueller, M.; Wang, M.; Schulze-Briese, C. Optimal Fine φ-Slicing for Single-Photon-Counting Pixel Detectors. *Acta Crystallogr. D Biol. Crystallogr.* **2012**, *68*, 42–56. [CrossRef] [PubMed]
27. Kabsch, W. XDS. *Acta Crystallogr. D Biol. Crystallogr.* **2010**, *66*, 125–132. [CrossRef]
28. Evans, P.R.; Murshudov, G.N. How Good Are My Data and What Is the Resolution? *Acta Crystallogr. Sect. D Biol. Crystallogr.* **2013**, *69*, 1204–1214. [CrossRef]

29. McCoy, A.J.; Grosse-Kunstleve, R.W.; Adams, P.D.; Winn, M.D.; Storoni, L.C.; Read, R.J. Phaser Crystallographic Software. *J. Appl. Crystallogr.* **2007**, *40*, 658–674. [CrossRef]
30. Emsley, P.; Cowtan, K. Coot: Model-Building Tools for Molecular Graphics. *Acta Crystallogr. Sect. D Biol. Crystallogr.* **2004**, *60*, 2126–2132. [CrossRef]
31. Adams, P.D.; Afonine, P.V.; Bunkoczi, G.; Chen, V.B.; Davis, I.W.; Echols, N.; Headd, J.J.; Hung, L.-W.; Kapral, G.J.; Grosse-Kunstleve, R.W.; et al. PHENIX: A Comprehensive Python-Based System for Macromolecular Structure Solution. *Acta Crystallogr. Sect. D* **2010**, *66*, 213–221. [CrossRef] [PubMed]
32. Long, F.; Nicholls, R.A.; Emsley, P.; Graæulis, S.; Merkys, A.; Vaitkus, A.; Murshudov, G.N. AceDRG: A Stereochemical Description Generator for Ligands. *Acta Crystallogr. Sect. D Struct. Biol.* **2017**, *73*, 112–122. [CrossRef] [PubMed]
33. Potterton, L.; Agirre, J.; Ballard, C.; Cowtan, K.; Dodson, E.; Evans, P.R.; Jenkins, H.T.; Keegan, R.; Krissinel, E.; Stevenson, K.; et al. CCP4i2: The New Graphical User Interface to the CCP4 Program Suite. *Acta Crystallogr. Sect. D Struct. Biol.* **2018**, *74*, 68–84. [CrossRef]
34. Liebschner, D.; Afonine, P.V.; Moriarty, N.W.; Poon, B.K.; Sobolev, O.V.; Terwilliger, T.C.; Adams, P.D. Polder Maps: Improving OMIT Maps by Excluding Bulk Solvent. *Acta Crystallogr. Sect. D Struct. Biol.* **2017**, *73*, 148–157. [CrossRef] [PubMed]
35. Chen, P.Y.T.; DeColli, A.A.; Freel Meyers, C.L.; Drennan, C.L. X-Ray Crystallography–Based Structural Elucidation of Enzyme-Bound Intermediates along the 1-Deoxy-D-Xylulose 5-Phosphate Synthase Reaction Coordinate. *J. Biol. Chem.* **2019**, *294*, 12405–12414. [CrossRef]
36. Querol, J.; Rodríguez-Concepción, M.; Boronat, A.; Imperial, S. Essential Role of Residue H49 for Activity of *Escherichia Coli* 1-Deoxy-D-Xylulose 5-Phosphate Synthase, the Enzyme Catalyzing the First Step of the 2-C-Methyl-D-Erythritol 4-Phosphate Pathway for Isoprenoid Synthesis. *Biochem. Biophys. Res. Commun.* **2001**, *289*, 155–160. [CrossRef]
37. Koes, D.R.; Baumgartner, M.P.; Camacho, C.J. Lessons Learned in Empirical Scoring with Smina from the CSAR 2011 Benchmarking Exercise. *J. Chem. Inf. Model.* **2013**, *53*, 1893–1904. [CrossRef] [PubMed]
38. Sanders, S.; Vierling, R.J.; Bartee, D.; DeColli, A.A.; Harrison, M.J.; Aklinski, J.L.; Koppisch, A.T.; Freel Meyers, C.L. Challenges and Hallmarks of Establishing Alkylacetylphosphonates as Probes of Bacterial 1-Deoxy-D-Xylulose 5-Phosphate Synthase. *ACS Infect. Dis.* **2017**, *3*, 467–478. [CrossRef]
39. Zhou, J.; Yang, L.; DeColli, A.; Freel Meyers, C.; Nemeria, N.S.; Jordan, F. Conformational Dynamics of 1-Deoxy-D-Xylulose 5-Phosphate Synthase on Ligand Binding Revealed by H/D Exchange MS. *Proc. Natl. Acad. Sci. USA* **2017**, *114*, 9355–9360. [CrossRef]
40. Beroza, P.; Crawford, J.J.; Ganichkin, O.; Gendelev, L.; Harris, S.F.; Klein, R.; Miu, A.; Steinbacher, S.; Klingler, F.-M.; Lemmen, C. Chemical Space Docking Enables Large-Scale Structure-Based Virtual Screening to Discover ROCK1 Kinase Inhibitors. *Nat. Commun.* **2022**, *13*, 6447. [CrossRef]
41. Yu, C.; Leung, S.K.P.; Zhang, W.; Lai, L.T.F.; Chan, Y.K.; Wong, M.C.; Benlekbir, S.; Cui, Y.; Jiang, L.; Lau, W.C.Y. Structural Basis of Substrate Recognition and Thermal Protection by a Small Heat Shock Protein. *Nat. Commun.* **2021**, *12*, 3007. [CrossRef]
42. Gierse, R.M.; Reddem, E.R.; Alhayek, A.; Baitinger, D.; Hamid, Z.; Jakobi, H.; Laber, B.; Lange, G.; Hirsch, A.K.H.; Groves, M.R. Identification of a 1-Deoxy-D-Xylulose-5-Phosphate Synthase (DXS) Mutant with Improved Crystallographic Properties. *Biochem. Biophys. Res. Commun.* **2021**, *539*, 42–47. [CrossRef]
43. Hartshorn, M.J.; Murray, C.W.; Cleasby, A.; Frederickson, M.; Tickle, I.J.; Jhoti, H. Fragment-Based Lead Discovery Using X-Ray Crystallography. *J. Med. Chem.* **2005**, *48*, 403–413. [CrossRef] [PubMed]
44. Patel, D.; Bauman, J.D.; Arnold, E. Advantages of Crystallographic Fragment Screening: Functional and Mechanistic Insights from a Powerful Platform for Efficient Drug Discovery. *Prog. Biophys. Mol. Biol.* **2014**, *116*, 92–100. [CrossRef] [PubMed]
45. Bartee, D.; Sanders, S.; Phillips, P.D.; Harrison, M.J.; Koppisch, A.T.; Freel Meyers, C.L. Enamide Prodrugs of Acetyl Phosphonate Deoxy-D-Xylulose-5-Phosphate Synthase Inhibitors as Potent Antibacterial Agents. *ACS Infect. Dis.* **2019**, *5*, 406–417. [CrossRef] [PubMed]

Disclaimer/Publisher's Note: The statements, opinions and data contained in all publications are solely those of the individual author(s) and contributor(s) and not of MDPI and/or the editor(s). MDPI and/or the editor(s) disclaim responsibility for any injury to people or property resulting from any ideas, methods, instructions or products referred to in the content.